# Spectroscopic properties of polyacetylene segments in copolymers

E. Mulazzi and A. Ripamonti
*Dipartimento di Fisica dell'Università di Milano and Istituto Nazionale Fisica della Materia, Via Celoria 16, 20133 Milano, Italy*

C. Godon and S. Lefrant
*Laboratoire de Physique Cristalline, Institut des Matériaux, 2 rue de la Houssinière, Boîte Postale 32229, 44322 Nantes Cedex 03, France*

(Received 1 December 1997; revised manuscript received 6 March 1998)

In this paper we present an extensive study of the optical properties of polyacetylene [$(CH)_x$ and $(CD)_x$] segments in copolymers by means of several spectroscopic techniques. They include UV-visible absorption, resonant Raman scattering, and photoinduced infrared absorption. A large variety of samples in either diblock or triblock copolymers, in general in the solid state, but also, in one particular case, in solution, are investigated. We show that the optical properties of these copolymers are strongly dependent on the distribution of conjugation lengths of segments in the different samples. A consistent model based on the vibrational and electronic properties of the polyacetylene conjugated segments and on a bimodal distribution is used to reproduce the band shapes observed in the UV-visible absorption, resonance Raman scattering, and photoinduced infrared-absorption spectra. The calculated structured shapes of the bands, and in particular the features in the low-frequency region of the photoinduced infrared absorption band in the different samples, are in very good agreement with the experimental data. [S0163-1829(98)06324-3]

## I. INTRODUCTION

Conducting polymers have been extensively studied these two last decades[1] for both fundamental research and technical application purposes. In this respect, the optical properties of such compounds have played an important role in the design of materials for application in different domains including electronics, nonlinear optics, and photonics.[2] A major requirement for these applications is the processing of the materials which is in general achieved by using adequate methods of synthesis. One of the specific routes to the preparation of conjugated polymers, which involves a precursor polymer step,[3,4] has proved to be rather powerful to obtain samples of easier processing and higher purity in comparison with those obtained by standard methods. This kind of procedure has been used to prepare, for example, highly oriented polyacetylene[4] and also copolymers containing polyacetylene segments.[5] As a matter of fact, the use of polymer-based composites, blends, or copolymers has attracted increased interest from the scientific community by combining the electronic properties of conjugated polymers to those of host matrices. In particular, mechanical properties, transparency in the visible range, or the fact of being soluble in common solvents have been widely exploited to process material with usable technical applications. In this context, diblock or triblock copolymers have been synthesized, made of polyacetylene $(CH)_x$ and polynorbornene (PN) or polystyrene (PS) segments. These saturated polymers do not interact with the conjugated segments of $(CH)_x$ whose electronic and optical properties are not modified. Consequently, $(CH)_x$ conjugated segments can be studied in a rather diluted form with a controlled length.

In this paper, we present the optical properties of the copolymers polyacetylene $(CH)_x$-polynorbornene[4] [referred to in the following as $(CH)_x$-PN], and polyacetylene $(CH)_x$-polystyrene[6] [referred to in the following as $(CH)_x$-PS] studied by means of UV-visible absorption, resonant Raman-scattering (RRS), and photoinduced infrared-absorption (PIA) spectroscopic techniques. Since the synthesis of such copolymers leads to polyacetylene blocks whose length can be controlled from short ($\sim 10N$, where $N$ is the number of double bonds) to long segments ($>100N$), the optical properties can therefore be studied as a function of the length distribution of polyacetylene segments. In addition, since the copolymers are soluble in common solvents, the different spectroscopic properties of these materials can also be investigated in solution, and these data can be compared to those obtained in solid-state form. All experimental data have been analyzed in the frame of a bimodal distribution model previously elaborated[7] to interpret the optical properties of polyacetylene, including optical-absorption, RRS, and PIA spectra. This model, based on electronic states and vibrational modes calculated for the conjugated segments of different length of $(CH)_x$ (Ref. 7) uses the bimodal Gaussian distribution introduced in Ref. 7 in order to weight the various contributions of the conjugated segments of different lengths in the optical responses. A similar model based on finite $(CH)_x$ segments with various length, and also using a bimodal distribution was introduced,[8] to interpret Raman data only. Our investigation includes, in addition, the calculations of optical and PIA band shapes. This analysis is of prior importance to understand better the electronic and vibrational properties of polyacetylene in terms of conjugation lengths and their distributions in the samples. In particular, this study provides a significant test for the model introduced for standard polyacetylene, since the copolymers investigated contain short conjugated segments in a controlled large concentration.

 

In Sec. II, we report the synthesis of triblock $(CH)_x$-PN-$(CH)_x$, diblock $(CH)_x$-PN, and $(CH)_x$-PS copolymers. In Sec. III, we show the experimental spectra of RRS, UV-visible optical absorption, and PIA of the copolymers listed above. In Sec. IV, the theoretical model and calculated shapes of the bands in RRS, optical-absorption, and PIA spectra of the different samples are presented. Discussions and conclusions are given in Sec. V.

## II. SYNTHESIS

Triblock copolymers $(CH)_x$-PN-$(CH)_x$ and diblock copolymers $(CH)_x$-PN were prepared according to a precursor route method as described in Refs. 5 and 9, using either a trifunctional or monofunctional metathesis catalyst. The procedure needs the preparation of a precursor polymer of polyacetylene which polymerizes via a ring opening metathesis polymerization, using W or Mo-carbene complexes as initiators starting from the 7,8-*bis* (trifluoromethyl) tricyclo [4, 2, 2, $0^{2,5}$]-deca-3,7,9-triene as the monomer. A solution of norbornene (bicyclo [2.2.1]hept-2-ene) is added in order to obtain the polynorbornene blocks whose degree of polymerization $m$ ranges from 400 to 500, corresponding to an average molecular weight of $\approx$40 000. The catalyst-to-monomer ratio can be adjusted to prepare various lengths of the precursor of polyacetylene, controlled by size exclusion chromatography. Typical thermal treatment at 140 °C for 40 min under a high dynamic vacuum converts the precursor units into polyacetylene segments. The precursor copolymers are soluble in common solvents like chlorobenzene, toluene, or dichloromethane, which allows one to prepare films on specific substrates for spectroscopic measurements of free-standing cast films. In the case of the diblock copolymer $(CH)_x$-PS, a different method was used, starting from a monomer PVS (phenyl vinylsulfoxide). The procedure consists of inducing the polymerization using a polystyrene carbanion. A thermal treatment then transforms the PVS into polyacetylene, leading to $(CH)_x$-PS diblock copolymers. Details of the synthesis can be found in Refs. 6 and 10.

## III. EXPERIMENTAL RESULTS

### A. UV-visible absorption

In this subsection, we describe the experimental UV-visible absorption features of the different kinds of copolymers investigated in this paper. They consist of triblock and diblock polyacetylene-polynorbornene $(CH)_x$-PN-$(CH)_x$ and $(CH)_x$-PN, diblock polyacetylene-polystyrene $(CH)_x$-PS, and deuterated polyacetylene-polynorbornene $(CD)_x$-PN. In these various samples, the conjugated polyacetylene segments are of different lengths. This can be qualitatively achieved by using the synthesis methods described in Sec. II. The main purpose of this study is to investigate the changes in the features of the absorption spectra of the different samples compared to those reported for standard polyacetylene.

In Fig. 1, we show the absorption curves corresponding to the different samples as indicated. In Fig. 1(a), we present experimental results for the triblock copolymer $(CH)_{88}$-PN-$(CH)_{88}$. The absorption maximum is peaked at 2.5 eV, and the overall shape is slightly different from that

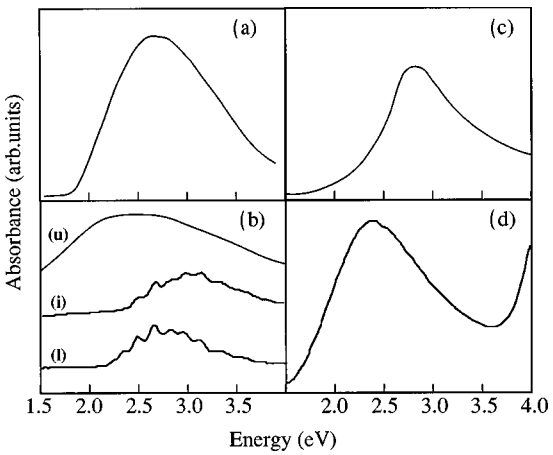


FIG. 1. Optical-absorption spectra of different types of copolymers recorded at room temperature. (a) Triblock $(CH)_x$-PN-$(CH)_x$. (b) Diblock $(CH)_x$-PN: ($u$) thin film ($N_{av}=40$); ($i$) thin film ($N_{av}=10$); ($l$) sample in solution ($N_{av}=10$). (c) Diblock $(CH)_x$-PS. (d) Diblock $(CD)_x$-PN in thin film.

observed in standard trans-$(CH)_x$ as shown in Fig. 2 of Ref. 11. Notice that other triblock copolymers of this type have shown very close experimental features.[12] Conversely, the diblock copolymers $(CH)_x$-PN can be synthesized with a much better control on the length of the $(CH)_x$ conjugated segments. This fact, on the one hand, allows one to achieve much shorter conjugated sequences, and, on the other hand, their distribution is much narrower than in the case of triblock copolymers. This is illustrated by the absorption curves shown in Fig. 1(b) for $40N_{av}$ (from now on, the values of $N$ as deduced experimentally, e.g., from size exclusion chromatography, must be considered as average values $N_{av}$) and $10N_{av}$, respectively (see also Ref. 13, and references therein). Note that the values of $N_{av}$ have been deduced from size exclusion chromatography measurements which determine the approximate value of the molecular weight for the precursor polymer. They only provide an indication of the average values $N_{av}$ for the whole chain, irrespective of conjugation interruptions. Note also that the absorption for the copolymer with $40N_{av}$ sequences is rather similar in shape to that of the triblock copolymer shown in Fig. 1(a), although slightly shifted in energy. Conversely, the absorption of the sample with $10N_{av}$ sequences exhibits structures whose resolution is different if the compound is in solution or in the solid-state form. Let us mention that the average position of the maximum shifts from $\approx$2.5 eV in the case of the structureless band of $40N_{av}$ compound to $\approx$3 eV in the $10N_{av}$ case.

Figure 1(c) presents the absorption of $(CH)_x$-PS obtained according to the method described in Sec. II. The maximum of the absorption is observed at $\simeq$2.7 eV (460 nm). The average conjugation length has not been estimated from the synthesis in this case, but the shape and maximum position of the band indicate that short conjugated segments are present in the sample with a broad distribution.[6] Finally, Fig. 1(d) exhibits the absorption curve of the $(CD)_x$-PN diblock copolymer. The maximum position is recorded at 2.42 eV, shifted by comparison to the absorption of standard polyacetylene.

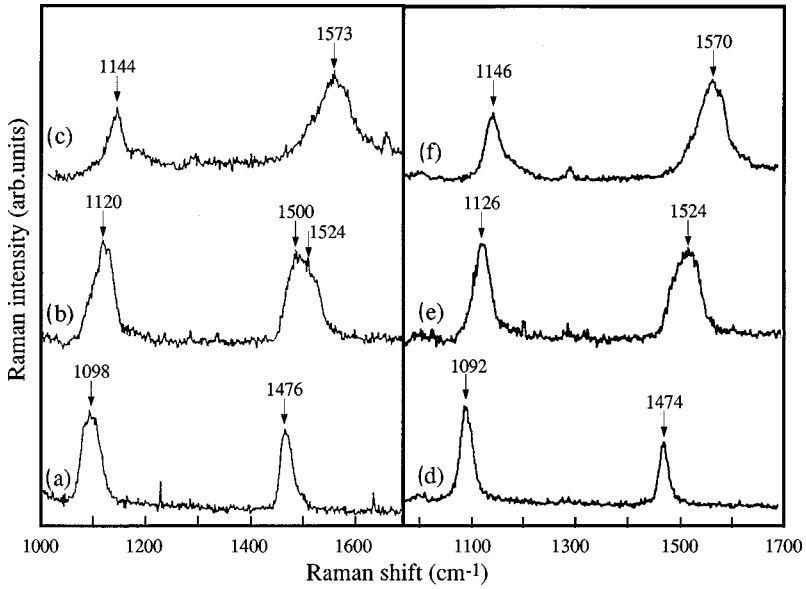


FIG. 2. RRS spectra of diblock copolymers recorded at room temperature for different excitation wavelengths. In (a), (b), and (c), RRS spectra of $(CH)_x$-PN ($N_{av} \simeq 100$) for $\lambda_L = 647.1$, 457.9, and 351.1 nm, respectively. In (d), (e), and (f), RRS spectra of $(CH)_x$-PS for the same $\lambda_L$, respectively.

### B. Resonant Raman scattering

Resonant Raman spectra of triblock copolymers $(CH)_x$-PN-$(CH)_x$ have been published previously in Refs. 11 and 14. It was reported that due to the small differences in the conjugation length of the $(CH)_x$ segments in the different samples studied, no significant change was observed in the RRS spectra. In addition, they were similar to the spectra of trans-$(CH)_x$ samples containing a significant amount of short segments.

In Fig. 2, we report the RRS spectra of two different diblock copolymers $(CH)_x$-PN, where the average lengths of the $(CH)_x$ segments are $N_{av} = 100$ and 10, respectively, as determined by molecular mass distribution of the precursor from size exclusion chromatography. Let us recall that optical and vibrational properties of $(CH)_x$ polymers are characteristic of noninterrupted conjugated segments, and therefore provide a way to determine their length distribution. Also, the RRS spectra of $(CH)_x$-PS are shown for comparison in the same Fig. 2.

In Figs. 2(a), 2(b), and 2(c) we present the RRS spectra of $(CH)_x$-PN for $N_{av} = 100$ for different excitation wavelengths ranging from $\lambda_L = 647.1$ to 351.1 nm. In Figs. 2(d), 2(e), and 2(f), RRS spectra of $(CH)_x$-PS are reported for the same $\lambda_L$. In both cases, the main features of these spectra are broad Raman bands peaked at 1098 and 1476 $cm^{-1}$ for the red light excitation (647.1 nm), shifted to 1144 and 1573 $cm^{-1}$, respectively, for the near-UV excitation (351.1 nm). These spectra are rather similar to those reported in Refs. 11 and 14 for triblock copolymers $(CH)_x$-PN-$(CH)_x$. Notice that no resolved two-band structure is observed for excitations in the violet and near-UV range (457 and 351.1 nm), as reported in the spectra of good trans-$(CH)_x$ (see Refs. 15 and 16). This result is an indication of the relatively low weight of long segments, compared to the short ones, in the bimodal distribution of conjugated lengths in the sample.[7] Note that the Raman spectra of $(CH)_x$-PS are rather similar to these described above for $(CH)_x$-PN with $N_{av} = 100$. This indicates that the average values of the conjugation lengths of $(CH)_x$ segments are very close in both the samples. This does not allow us to extrapolate the value of $N_{av}$ in $(CH)_x$-PS, since the presence of defects may play an important role in the interruption of the conjugation length.

In Fig. 3, we report the RRS spectra of the diblock copolymer $(CH)_x$-PN with $N_{av} = 10$ in solid state form [Figs. 3(a), 3(b), and 3(c)], and in solution of dicloromethane [Figs. 3(d), 3(e), and 3(f)] for the different excitation wavelengths. Note that, in this latter case, we show only the bands in the frequency range 1400–1600 $cm^{-1}$. These results have been taken from Ref. 17.

The most peculiar result in these spectra is the appearance of a well-resolved structure in the near-UV range excitation in both solid state and solution [Figs. 3(c) and 3(f)]. This is illustrated in particular by the peaks at 1529 and 1565 $cm^{-1}$ [Fig. 3(c)] and at 1536 and 1558 $cm^{-1}$ [Fig. 3(f)]. This well-resolved structure is also observed for $\lambda_L = 457.9$ nm from the sample in solution [Fig. 3(e)], but, unexpectedly, it disappears in the RRS spectrum from the sample in solid-state form, for the same $\lambda_L$ [Fig. 3(b)]. Conversely, the RRS band peaked at 1538 $cm^{-1}$ is rather narrow. For the excitation in the red range we observe, in both cases, downshifted weak and broad bands at 1476 and 1094 $cm^{-1}$ for the sample in solid-state form [Fig. 3(a)], and at 1505 $cm^{-1}$ for the sample in solution [Fig. 3(d)].

In Fig. 4, we show the RRS spectra of deuterated $(CD)_x$-PN diblock copolymers recorded for different excitation wavelengths from the red to UV range. Notice that the purpose for investigating the $(CD)_x$-PN copolymer was twofold: (i) to achieve the synthesis of $(CD)_x$ segments of controlled lengths as in $(CH)_x$ copolymer samples; and (ii) to achieve a synthesis of partially aligned $(CD)_x$ segments. Concerning point (i), it is possible to infer from the figures that the bands in these spectra show the same features as observed above in diblock $(CH)_x$-PN in solid-state form. In fact the bands are much narrower, and their peak positions

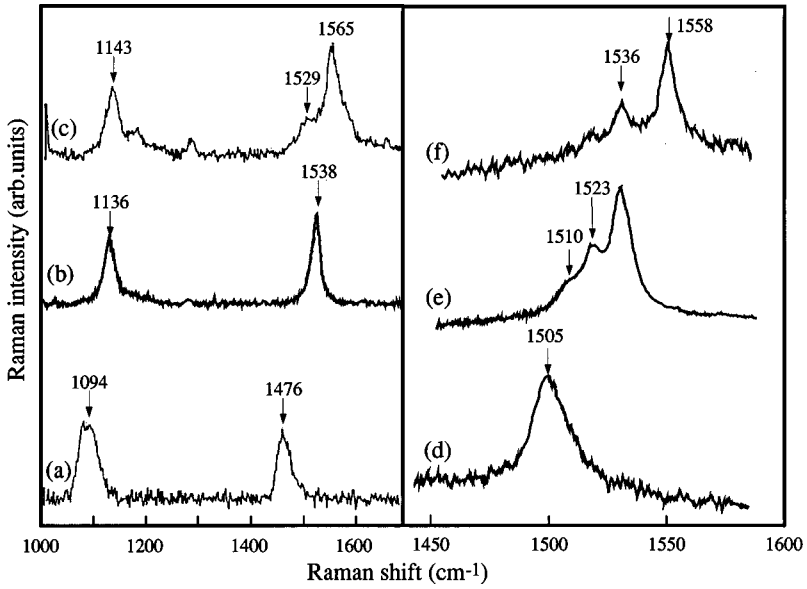


FIG. 3. RRS spectra recorded at room temperature of diblock $(CH)_x$-PN copolymers. In (a), (b), and (c), RRS spectra of thin-film sample ($N_{av}=10$) for $\lambda_L=647.1$, 457.9, and 351.1 nm, respectively. In (d), (e), and (f), RRS spectra in solution of dichloromethane ($N_{av}=10$) in the range 1450–1600 $cm^{-1}$ for $\lambda_L=568.2$, 457.9, and 406.7 nm, respectively.

shift to higher frequencies with respect to those recorded in the spectra of standard trans-$(CD)_x$. In particular from Figs. 4(a)–4(c), one can observe that the frequency of the peak of the double bond stretching mode band increases from 1370 $cm^{-1}$ (for $\lambda_L=676.4$ nm) to 1503 $cm^{-1}$ (for $\lambda_L=363.8$ nm). This is a clear indication that very short conjugated segments are present in the sample, much shorter than in standard $(CD)_x$.[15] Note also that, as found in standard trans-$(CD)_x$, the peak of the band of the single bond stretching mode undergoes a much smaller shift when the excitation wavelength changes as indicated above, because the frequency of this mode is almost independent of the segment length. In regards to point (ii), although RRS experiments performed in polarized light were unsuccessful due to storage conditions in a vacuum tube, polarized IR-absorption measurements confirm the partial orientation of the $(CD)_x$ segments in the copolymer.

### C. Photoinduced infrared-absorption spectra

Photoinduced infrared-absorption spectra of different triblock copolymers $(CH)_x$-PN-$(CH)_x$ have been already published.[18,19] They are shown again in Figs. 5(a) and 5(b) for comparison with the PIA spectra of diblock copolymers [Fig. 5(c)]. As already pointed out,[18,19] the two vibrational photoinduced bands peaked at 1370 and 1287 $cm^{-1}$ do not depend on the sample investigated. This is also confirmed in the PIA spectra for $(CH)_x$-PN diblock copolymers [see Figs. 5(a) and 5(c)]. In the case of a deuterated $(CD)_x$-PN copolymer, the equivalent features [whose intensity ratio is the opposite of that observed in $(CH)_x$] (Refs. 20–23) are reported at 1045 and 1225 $cm^{-1}$ [Fig. 5(d)] at the same values as recorded in the PIA spectra of Refs. 20–22 of deuterated polyacetylene. Conversely, the broad band observed in $(CH)_x$-PN copolymers in the ranges 500–1000 and 400–900 $cm^{-1}$ in $(CD)_x$-PN copolymers is sample dependent.[18,19] In particular, in $(CH)_x$-PN-$(CH)_x$ triblock copolymers, the broad band clearly exhibits components at 620 and 738 $cm^{-1}$ [Fig. 5(a)] which are shifted and better resolved at 520 and 700 $cm^{-1}$ [Fig. 5(b)] when the weight of short conjugated segments increases. The band in Fig. 5(a) is very similar to the one observed in standard polyacetylene.[18] Conversely, in the case of $(CH)_x$-PN with $N_{av}\simeq 12$, the band can be interpreted as an envelope of several components peaked at 600, 700, and 800 $cm^{-1}$ in the frequency range 600–900 $cm^{-1}$. For the diblock $(CD)_x$-PN copolymers with $N_{av}\sim 20$, the analogous band, broad and structureless, is peaked at 550 $cm^{-1}$ and well shifted with respect to the standard $(CD)_x$ band, peaked at 400 $cm^{-1}$ (Refs. 20–22).

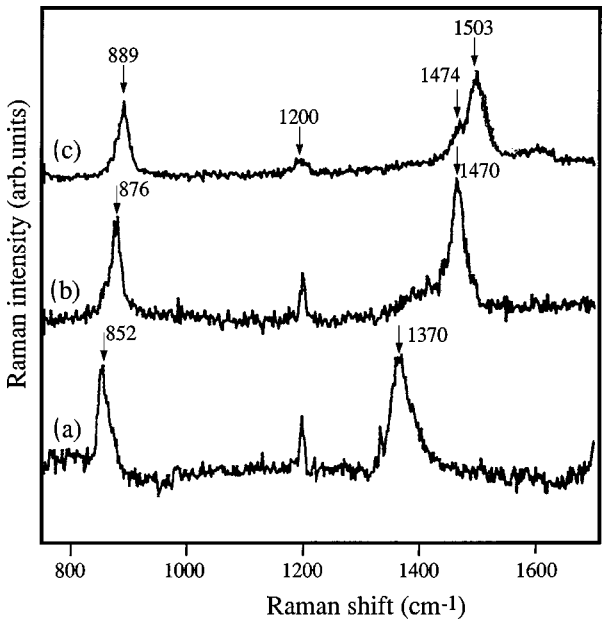


FIG. 4. RSS spectra recorded at room temperature of diblock copolymer $(CD)_x$-PN: (a) $\lambda_L=676.4$ nm, (b) $\lambda_L=457.9$ nm, and (c) $\lambda_L=363.8$ nm.

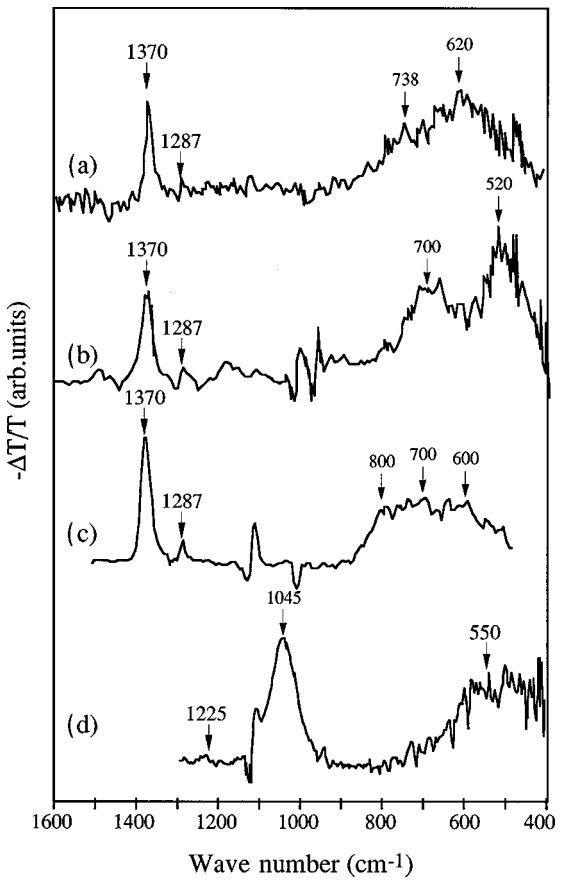


FIG. 5. Photoinduced infrared-absorption spectra recorded at 77 K with an excitation wavelength $\lambda_L = 514.5$ nm. The pump beam is polarized perpendicular to the stretching axis, while the photoinduced infrared absorption spectrum is polarized parallel to the chain axis: (a) $(CH)_{88}$-PN-$(CH)_{88}$, (b) $(CH)_{75}$-PN-$(CH)_{75}$, (c) $(CH)_x$-PN with $N_{av} \simeq 12$, and (d) $(CD)_x$-PN with $N_{av} \simeq 20$.

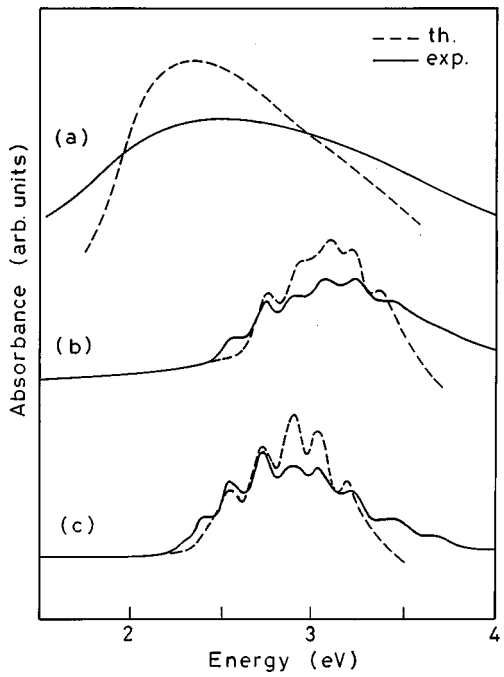


FIG. 6. Comparison between experimental (continuous line) and calculated (dashed line) optical-absorption band shapes. (a) and (b) Solid-state samples with $N_{av} = 40$ and 10, respectively. (c) Sample in solution with $N_{av} = 10$. The parameters used in the calculations are given in Table I.

## IV. THEORETICAL RESULTS

Here we present calculated band shapes to be compared with those recorded in the spectra obtained by using various spectroscopic techniques (UV-visible absorption, RRS, and PIA) from different copolymer samples as described in Sec. III. The basic idea of these calculations is to show that the model introduced in Ref. 7, in order to calculate the band shapes in the RRS, optical-absorption, and PIA (Refs. 18, 19, and 23) spectra for polyacetylene samples is also able to simulate analogous bands in the related spectra of copolymers with polyacetylene segments. Moreover, our purpose is to prove that, in these copolymers (in solid-state form and in solution), the conjugated segment distributions found to simulate the optical absorption in one copolymer are very similar to those found for the band shapes observed in the spectra of the RRS and PIA of the same sample. Then the main differences between the experimental band shapes of triblock copolymers, diblock copolymers, and polyacetylene systems are mainly explained in terms of different distributions of conjugated segments. This is expected from the values of $N_{av}$ deduced from the synthesis, as reported in Sec. III.

The band shapes of optical absorption and Raman scattering of the triblock copolymers are very similar to those found in polyacetylene samples, as has been already described in Sec. III. Here we do not show these band shapes, as the distributions of conjugated segments found to simulate the experimental results were already reported in Ref. 14.

Conversely, we show the optical-absorption band shapes of diblock copolymers given in Fig. 6, where the experimental data are also reported for comparison [they are the same as given in Fig. 1(b)]. The distribution parameters used to calculate the band shapes are given in Table I. Notice that the broad band in Fig. 6(a), which is similar to that observed in the optical-absorption spectra of triblock copolymers, reproduces the experimental data well by using a bimodal distribution centered on long and short segments, as in polyacetylene samples. Conversely, a good agreement is obtained between the calculated multistructured band shapes given in Figs. 6(b) and 6(c) and the experimental data by using the bimodal distribution parameters centered on short segments only. This can be derived from the values of $N_1$ and $N_2$ in Table I. Moreover, the weight of the distribution centered on $N_2$, which is $(1-G)$, is always larger than the other one centered on $N_1$, which is $G$. The values of the parameters determine a distribution characterized only by one peak on the shorter segments and a very asymmetric shape with a tail

TABLE I. Parameters used to calculate the band shapes given in Figs. 6, 7, 8, and 9.

| Figure | $N_1$ | $\sigma_1$ | $N_2$ | $\sigma_2$ | $G$ | $\gamma$ |
|---|---|---|---|---|---|---|
| Fig. 6(a) | 40 | 10 | 12 | 6 | 0.45 | 0.08 |
| Figs. 6(b) and 8 | 10 | 5 | 5 | 1 | 0.40 | 0.08 |
| Figs. 6(c) and 8 | 10 | 5 | 5 | 1 | 0.35 | 0.018 |
| Fig. 9 | 14 | 5 | 5 | 2 | 0.5 | 0.08 |

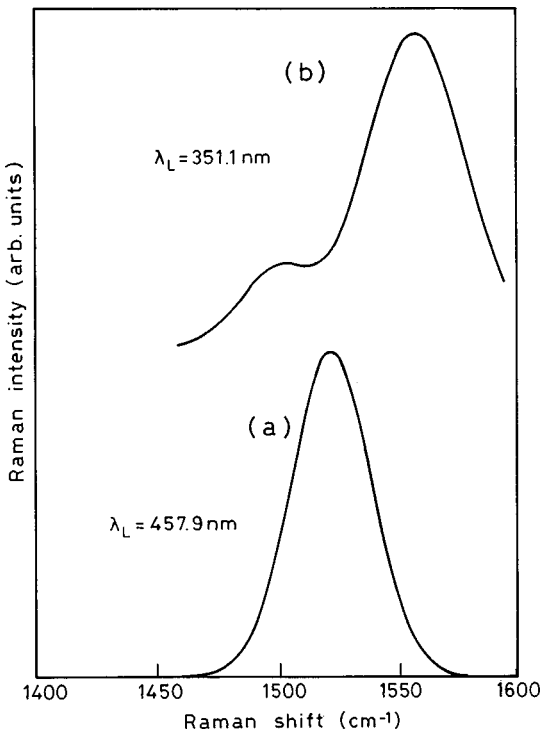


FIG. 7. Calculated RRS band shapes in the frequency range 1400–1600 $cm^{-1}$ of $(CH)_x$-PN (solid-state sample with $N_{av}=10$). (a) $\lambda_L=457.9$ nm and (b) $\lambda_L=351.1$ nm. The parameters used in the calculations are given in Table I. These band shapes have to be compared with those of Figs. 3(b) and 3(c), respectively.

toward longer conjugated sequences. Notice that the values found for $N_1$ and $N_2$ are consistent with the average value $N_{av}=10$ determined from the synthesis. The numerous peaks in the structured bands in Figs. 6(b) and 6(c) represent the different contributions of the electronic transitions related to the conjugated segments which have more weight in the short segment distribution, also taking into account the decrease, as a function of $N$, of the electric dipole moment intensities, as reported in Ref. 7. The different resolution of the structures is determined in the calculation by the value of $\gamma$ which is proportional to the inverse of the lifetime of the electronic states of the copolymers in solid-state form and in solution. The values of $\gamma$ given in Table I indicate that the lifetime of the electronic states is longer when the system is in solution with respect to the case of the solid-state form.

By using the same set of parameters, we have performed calculations of the RRS band shapes observed in the spectra of the two copolymers characterized by the absorption given in Figs. 6(b) and 6(c). In Figs. 7(a) and 7(b) we give the band shapes for the double bond vibrational modes of the diblock in solid-state form for $\lambda_L=457.9$ and 351.1 nm. These band shapes have to be compared with those given in Figs. 3(b) and 3(c) ($N_{av}=10$). These features are much narrower than those observed in standard polyacetylene (see Refs. 7 and 16), and are mainly determined by the narrow distribution of short conjugated segments, as given in Table I.

In Figs. 8(a)–8(d), we report the calculated band shapes of RRS spectra of the diblock copolymer in solution for different exciting wavelengths as indicated ($\lambda_L=568.2$, 488, 431.1, and 406.7 nm, respectively). The experimental data taken from Ref. 17, and some of them, already given in Figs. 3(d)–3(f), are also included in the figure, for comparison, with the calculated band shapes. The most striking result which can be derived from these figures is related to the fact that the band shapes are very narrow, much narrower than those given in Fig. 7, and with several structures. In order to obtain the calculated band shapes, we have also changed the parameter $\Delta_N$ related to the broadening of the double-bond modes (see Ref. 7), from the usual value used in standard polyacetylene and copolymers in solid-state form ($\Delta_N$

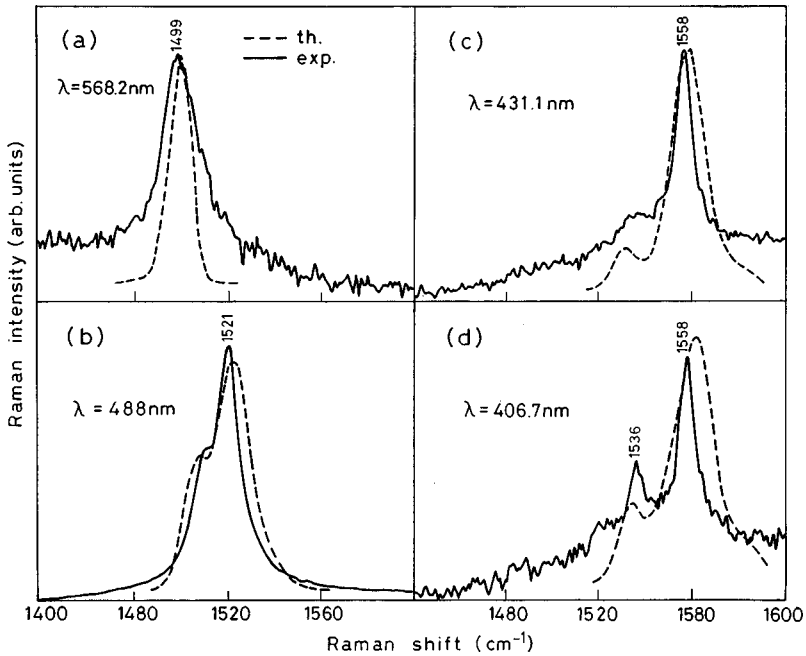


FIG. 8. Comparison between experimental (continuous line) and calculated (dashed line) RRS band shapes in the frequency range 1400–1600 $cm^{-1}$ of $(CH)_x$-PN (sample in solution and $N_{av}=10$). (a) $\lambda_L=568.2$ nm, (b) $\lambda_L=488$ nm, (c) $\lambda_L=431.1$ nm, and (d) $\lambda_L=406.7$ nm. The parameters used in the evaluations are given in Table I.

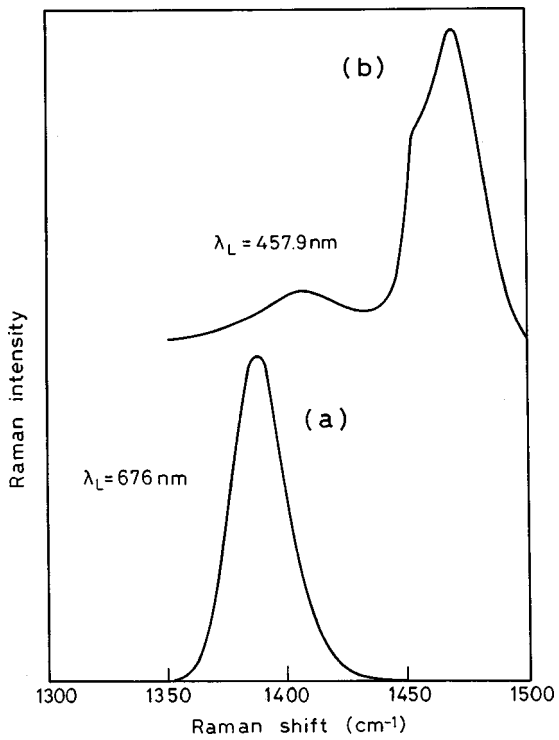


FIG. 9. Calculated RRS band shapes in the frequency range 1300–1500 $cm^{-1}$ of $(CD)_x$-PN: (a) $\lambda_L = 676$ nm and (b) $\lambda_L = 457.9$ nm. The parameters used in the evaluations are given in Table I. These band shapes have to be compared with those of Figs. 4(a) and 4(b), respectively.

$=14\ cm^{-1}$) to the value $\Delta_N = 8\ cm^{-1}$. Then the peak positions and other features in the band shapes, in agreement with the experimental data, are determined by the different contributions of the double-bond vibrational modes of the segments more weighted in the distributions.

Notice that both the values of $\gamma$ and $\Delta_N$ change significantly from those found in standard polyacetylene with respect to the case of $(CH)_x$ segments in solution. This result can be expected from a system in which the interactions of the electronic and vibrational states with the surrounding states are smaller compared to a solid-state system.

In Fig. 9, we give the Raman band shapes for the double-bond vibrational modes of deuterated diblock copolymer $(CD)_x$-PN for $\lambda_L = 676$ and 457.9 nm, using the distribution given in Table I. These results have to be compared with the experimental band shapes given in Figs. 4(a) and 4(b). Again the narrow distribution, determined by the parameters used, is responsible for the narrow band shapes with structures. As can be seen from this figure, the large shift observed experimentally in the double-bond frequencies from $\lambda_L = 676.4$ and 457.9 nm [see Figs. 4(a) and 4(b)] is well accounted for theoretically. This is expected, as already mentioned, since the frequency of this mode is strongly dependent on the length of the conjugated segments.[24]

In Fig. 10, we report the band shape of the broad band observed in the vibrational PIA spectra in the frequency range 400–1000 $cm^{-1}$ in the copolymers containing $(CH)_x$ and $(CD)_x$ segments. The band shapes were calculated by using the model of Refs. 18, 19, and 23. As we discussed in Sec. III, this band shape changes dramatically as a function of the length of conjugated segments which have more

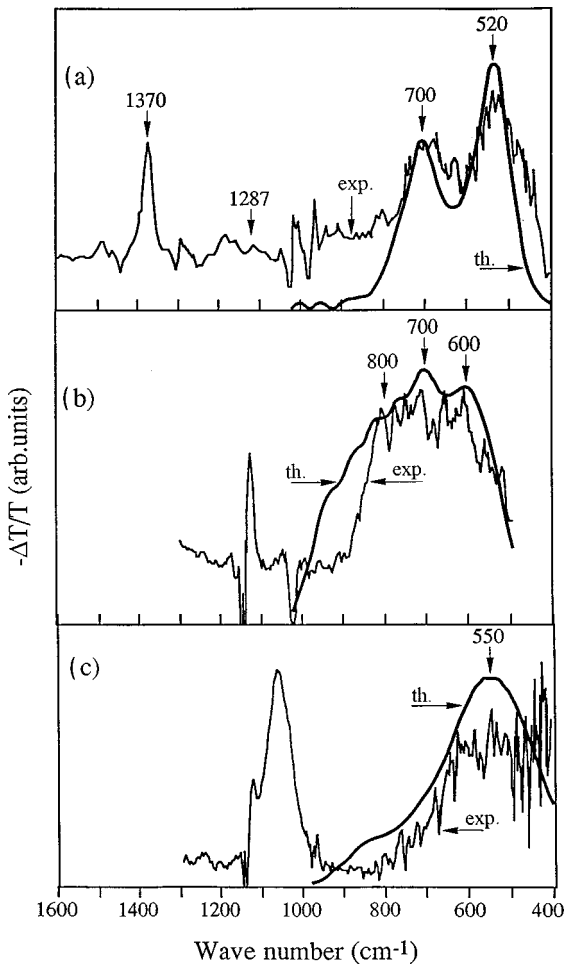


FIG. 10. Calculated PIA band shapes in the frequency range 400–1000 $cm^{-1}$: (a) triblock copolymer $(CH)_{75}$-PN-$(CH)_{75}$, (b) diblock copolymer $(CH)_x$-PN, and (c) diblock copolymer $(CD)_x$-PN. The experimental data are also shown for comparison. The parameters used in the evaluations are given in Table II.

weight in the distribution. Also, the intensity of the dipole moments, decreasing with $N$ (see Ref. 19), plays an important role in such a calculation. In Table II, we give the parameters used in these calculations.

The most striking result is related to the fact that when, in the bimodal distribution, $N_1$ is centered on long segments and $N_2$ on short ones, the broad band presents a principal peak and a secondary one. This last feature becomes more evident whenever the weight of the short segment distribution becomes predominant. This is the case given in Fig. 10(a) for the triblock copolymer $(CH)_{75}$-PN-$(CH)_{75}$.

A different case is reported in Fig. 10(b), where the broad band presents different structures at ~600, 700, and

TABLE II. Parameters used to calculate the band shapes given in Fig. 10.

| Figure | $N_1$ | $\sigma_1$ | $N_2$ | $\sigma_2$ | $G$ |
|---|---|---|---|---|---|
| Fig. 10(a) | 50 | 10 | 13 | 5 | 0.35 |
| Fig. 10(b) | 14 | 6 | 8 | 2 | 0.5 |
| Fig. 10(c) | 20 | 8 | 13 | 5 | 0.5 |

800 $cm^{-1}$. The calculated band shapes, which reproduce rather well the experimental broad and structured band, has been obtained by using the parameters given in Table II, which indicate that $N_1$ and $N_2$ are both centered on short segments. The well-defined structures in the band shape are due to the different contributions of the photoinduced vibrational frequencies of the short segments, which are more heavily weighted in the distribution. This result is analogous to what was found (mutatis mutandis) in the case of the optical absorption and RRS band shapes for the diblock copolymers with $N_{av}=10$ in solid state form.

In Fig. 10(c), we report the shape of the broad band in the PIA spectra of the $(CD)_x$-PN copolymer, calculated by using the parameters given in Table II. Notice that, in this case, since the values of $N_1$ and $N_2$ determine a distribution more shifted toward intermediate lengths, the low-frequency band becomes structureless and broad, the maximum being peaked at 550 $cm^{-1}$, well displaced with respect to the value found in standard $(CD)_x$ polyacetylene.[20–22]

## V. DISCUSSION AND CONCLUSION

In this paper we have presented experimental spectra of optical absorption, RRS, and PIA of polyacetylene-based copolymers containing polyacetylene segments, and a theoretical analysis and interpretation of these data. The main purpose of the synthesis of these copolymers was to prepare samples with $(CH)_x$ segments of controlled conjugation lengths, in some cases aligned along the chain axis. The aim of the present investigation was therefore an extensive characterization of these copolymers in terms of conjugation lengths of the segments in the polymeric chains. This was achieved via a study of the main spectroscopic optical properties of the samples, derived from different techniques and through the investigation of the changes of the spectroscopic features with the conjugation lengths of the segments in the different copolymers. This is an important issue since, as discussed in Sec. III, the size exclusion chromatography measurements (performed after the synthesis of the precursor polymer block) provide only a rather approximate value of $N_{av}$ of the overall chain. Conversely, the spectroscopic features are determined by the electronic and vibrational properties of noninterrupted conjugated segments along the polymeric chains.

In order to obtain a coherent picture and characterization of a specific copolymer, the optical spectroscopic features have been investigated by means of different techniques on the same sample. In such a way, it is possible to give an interpretation of the experimental results from a specific compound by using a consistent model which includes the electronic and vibrational properties of the ground and excited states of the conjugated segments of different length (see Refs. 7, 18, and 19).

As we have shown in Secs. III and IV, the dramatic changes observed in the spectroscopic data of optical absorption, RRS, and PIA in the two block copolymers, with respect to the triblock ones, are very well accounted for, through different distributions of conjugated segments.

In fact, the data of the triblock copolymers are interpreted in terms of a broad bimodal distribution centered on long and short conjugated segments. The various peculiarities observed in the spectra of these copolymers are explained (see Secs. III and IV) by considering the different weights of the long segments with respect to the short ones. This result is in rather good agreement with experimentally estimated $N_{av}$ values determined in the synthesis by size exclusion chromatography ($N_{av}\sim 88$ and $\sim 75$). In the case of diblock copolymers characterized by a smaller and more controlled $N_{av}$ value ($N_{av}\sim 10$), all spectroscopic data exhibit much sharper features due to the separate contributions of various short segments. As a consequence, the distributions, which are derived from the theoretical evaluation, are centered only on short segments. In this situation, the bimodal distribution becomes a very asymmetric one with a tail toward the long segment side. Note also that, from the distributions and the values of the parameters used in the calculations, one can determine theoretical values of $N_{av}$ which are in agreement with those evaluated from the synthesis for the different samples.

To summarize, we have presented a series of optical spectroscopic data of different types of copolymers containing polyacetylene segments of different lengths. All these data have been interpreted in a coherent way with a theoretical model, which also turns out to be successful when short segments are present in the sample. In addition, this model has also been applied to Durham-type polyacetylene samples characterized only by short segments, and the features of PIA spectra of these samples have been found in agreement with the experimental data.[25]

## ACKNOWLEDGMENTS

Triblock and diblock $(CH)_x$-PN copolymer samples have been synthesized at the Technische Universität of Graz (Austria) while the samples $(CH)_x$-PS at the Institut Charles Sadron in Strasbourg (France). Dr. F. Stelzer and Dr. G. Leising of the Technische Universität of Graz, and Dz. C. Mathis of the Institut Charles Sadron of Strasbourg, are gratefully acknowledged. The Institut des Materiaux is Unité Mixte de Research CNRS-Université de Nantes n. 6502.

[1] See, for example, Proceedings of the International Conference on Synthetic Metals, Snowbird, 1996 [Synth. Met. **84–86 (1997)**].

[2] See, for instance, *Science and Applications of Conducting Polymers*, edited by W. R. Salaneck, D. T. Clark, and E. J. Samuelson (Hilger, Bristol, 1990).

[3] J. H. Edwards, W. J. Feast, and D. C. Bott, Polymer **25**, 295 (1984).

[4] F. Stelzer, W. Fisher, G. Leising, and C. Heller, in *Electronic Properties of Conjugated Polymers*, edited by H. Kuzmany, M. Mehering, and S. Roth, Springer Series in Solid State Science, Vol. 107 (Springer-Verlag, Berlin, 1992), p. 231.

[5] S. A. Krouse and R. R. Schrock, Macromolecules **21**, 1885 (1988).

[6] D. Reibel, Ph.D. thesis, University Louis Pasteur, Strasbourg, 1994.

[7] G. P. Brivio and E. Mulazzi, Phys. Rev. B **30**, 876 (1984).

[8] H. Kuzmany, Phys. Status Solidi B **97**, 521 (1980); Pure Appl. Chem. **57**, 235 (1985).
[9] G. Leising, F. Stelzer, and H. Kalhert, J. Phys. (Paris), Colloq. **44**, C3-139 (1983).
[10] R. S. Kanga, T. E. Hogen-Esch, E. Raidrianalimanana, A. Soum, and M. Fontanille, Macromolecules **23**, 4241 (1990).
[11] S. Lefrant, T. Verdon, E. Mulazzi, and G. Leising, in *Frontiers of Polymer Research*, edited by P. N. Prasad and J. K. Nigam (Plenum, New York, 1991), p. 105.
[12] T. Verdon, Ph.D. thesis, University of Nantes, 1990.
[13] E. Mulazzi, A. Ripamonti, C. Godon, and S. Lefrant, Synth. Met. **69**, 671 (1995).
[14] E. Mulazzi, G. Leising, F. Stelzer, T. Verdon, and S. Lefrant, Synth. Met. **41**, 1333 (1991).
[15] S. Lefrant, J. Phys. (Paris), Colloq. **44**, C3-247 (1983).
[16] E. Mulazzi, G. P. Brivio, E. Faulques, and S. Lefrant, Solid State Commun. **46**, 851 (1983).
[17] C. Heller, G. Leising, C. Godon, S. Lefrant, W. Fisher, and F. Stelzer, Phys. Rev. B **51**, 8107 (1995).
[18] E. Mulazzi, A. Ripamonti, T. Verdon, and S. Lefrant, Phys. Rev. B **45**, 9439 (1992).
[19] E. Mulazzi, A. Ripamonti, and S. Lefrant, Solid State Commun. **83**, 521 (1992).
[20] G. B. Blanchet, C. R. Fincher, F. C. Chung, and A. J. Heeger, Phys. Rev. Lett. **50**, 1938 (1983).
[21] Z. Vardeny, J. Orenstein, and G. L. Baker, Phys. Rev. Lett. **50**, 2032 (1983).
[22] H. E. Schaffer, R. H. Friend, and A. J. Heeger, Phys. Rev. B **36**, 7537 (1987).
[23] G. P. Brivio and E. Mulazzi, Solid State Commun. **60**, 203 (1986).
[24] R. Tiziani, G. P. Brivio, and E. Mulazzi, Phys. Rev. B **31**, 4015 (1985).
[25] E. Mulazzi, A. Ripamonti, C. Godon, S. Lefrant, and G. Leising, Synth. Met. **84**, 911 (1997).